Some numerical calculations of the vertical velocity field in hurricanes

By T. N. KRISHNAMURTI, *Department of Meteorology, University of California, Los Angeles*

(Manuscript received July 21, revised version October 30, 1961)

ABSTRACT

The commonly observed crescent-shaped geometry of the tangential wind field in hurricanes is imposed on the primitive equations of atmospheric motion, and solutions for the vertical velocity field are obtained. It is shown that the numerically computed vertical motion field exhibits a spiral form, very similar to what is observed in radar pictures in individual hurricanes.

Aircraft flight data from the National Hurricane Research Project are utilized to carry out the numerical calculations in several hurricanes over the Atlantic.

An attempt is made to obtain an analytic solution for the same complete system of equations for a generalized Rankine vortex with a prescribed crescent-shaped geometry. It is shown that the analytic solution has an interesting spiral form. This solution for the Rankine vortex is compared with the corresponding finite difference solution to estimate the errors in the finite difference solution.

1. Introduction

A method for obtaining the vertical motion field for a steady symmetric hurricane with a prescribed tangential motion was proposed by the author (Krishnamurti, 1961). This method will be outlined here and it will be shown how one can extend the analysis to obtain the vertical velocity field in an asymmetric hurricane with a prescribed tangential motion.

It will be one of the aims here to see if the numerical calculations can reproduce some of the observed features like the eye, the eye wall and the spiral bands in the vertical motion field.

Careful analysis of the cloud and radar pictures by meteorologists like Wexler (1947) and Jordan (1960) have given us some ideas about the dimensions and structure of the vertical motion field. The National Hurricane Research Project at Miami, Florida, has provided a considerable amount of aircraft flight data in recent years, and this has enabled us to understand the structure of the hurricane much better than in prior times.

The recent work of Berkofsky (1960) and Kasahara (1960) is perhaps the very few approaches in which hurricane development is treated as an initial value problem. It is the aim of all research workers to see the complete development of a hurricane in a model where one integrates the non-linear equations of motion and brings about many of the observed features. The present calculation of vertical motion is obtained from a complete system of equations and the treatment will be thus somewhat like obtaining vertical motions from the so-called diagnostic vertical velocity equation in the quasi-geostrophic vorticity system. Here we shall use the primitive equations and avoid the quasi-geostrophic assumptions that are perhaps not reasonable for a hurricane, where rather large ageostrophic motions have been demonstrated by many meteorologists over the past few years.

Since the calculations are made for a diagnostic type of system, the results may not be expected to be as startling as those one would obtain from an initial-value problem. Nevertheless, it would be of interest to see what sort of vertical motions are found when the observed tangential velocity field in hurricanes is imposed on the equations of motion. Figs. 1 and 2 show the typical tangential wind field in a hurricane. These were obtained from aircraft flight data of the National Hurricane Research Project at Miami. It may be mentioned here that the flights cover the area shown rather completely and the tangential

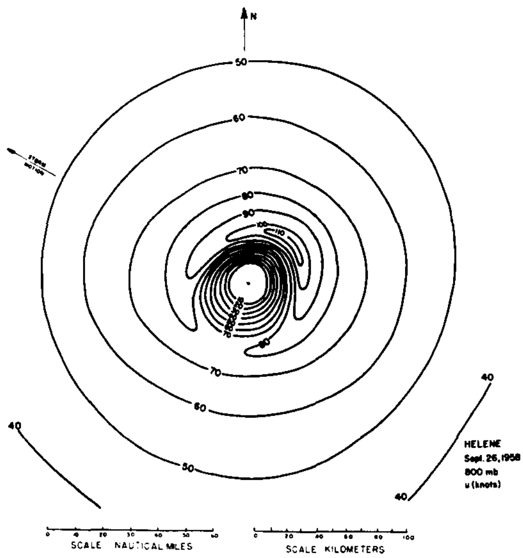

FIG. 1. The tangential wind velocity field in Hurricane Helene. 800 millibars. Units (knots). September 26, 1958.

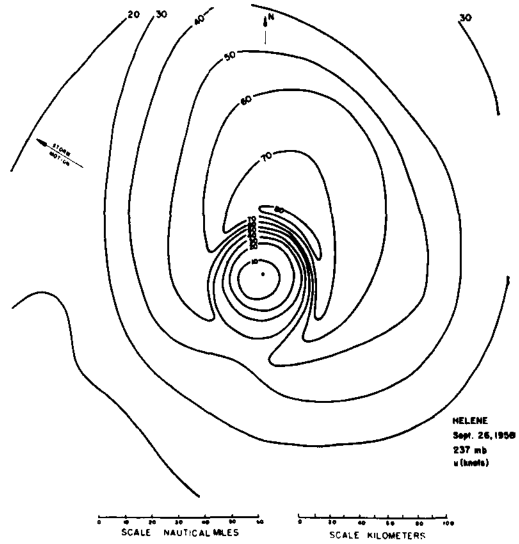

FIG. 2. The tangential wind velocity field in Hurricane Helene. 237 millibars. Units (knots). September 26, 1958.

wind field is one of the best observed fields. It has never been possible to obtain any reasonable vertical motion fields by the so-called kinematic technique because the horizontal divergence field of the observed wind field is not well defined. Figs. 1 and 2 were obtained from flights into Hurricane Cleo of 1958. The same crescent-shaped geometry is observed in all hurricane flight data.

We will now give an outline of the earlier work on the steady symmetric system (KRISHNAMURTI, 1961).

2. The steady symmetric hurricane

Cylindrical isobaric coordinates will be used with the radius vector r pointing outward, θ the angle increasing in the cyclonic sense. Table 1 lists the symbols used in this paper.

In KRISHNAMURTI (1961), the author examined the structure of a steady symmetric hurricane. Starting with the steady state Navier-Stokes equations it was shown that, for a prescribed u, the tangential motions field, a solution for the vertical motion field may be obtained by an application of a method of characteristics. Numerical calculations were made for different magnitudes of eddy momentum exchange coefficients.

It was found that, even for simple non-dimensional values of ν and $\varkappa$ (0.1 for instance), rather interesting solutions for v, ω, z, T and H showed up. The vertical motion field had an eye with sinking motion, very large upward motion at the eye wall and much weaker upward vertical motion at large distances from the center. The dimension and magnitudes of v, ω, z, T and H appeared reasonable when compared with certain observed magnitudes. Much still needed to be said about the magnitudes of ν and $\varkappa$. In this case it was found that the final pattern of ω was largely determined by the lateral eddy exchange of momentum. The role of vertical eddy exchange of momentum, though small in the determination of the vertical motion field, appeared significant for exchanges of momentum with the ground.

We shall here introduce the complete asymmetric system of equations and show how one can obtain a similar ω-equation and carry out the integrations for v, ω, z, T and H.

3. The asymmetric system of equations

The Navier-Stokes equations in cylindrical coordinates have been used by several meteorologists in their treatment of the hurricane problem; reference may be made to the contributions by KASAHARA (1960) and KUO (1959). We shall introduce as before two momentum exchange coefficients ν and $\varkappa$, where ν will be a coefficient for horizontal exchange and $\varkappa$, one for vertical exchange. The equations of motion, continuity and the first law of thermodynamics are written in the form:

$$\frac{\partial u}{\partial t}+u\frac{\partial u}{r\partial\theta}+v\left(\frac{\partial u}{\partial r}+\frac{u}{r}+f\right)+\omega\frac{\partial u}{\partial p}$$
$$=-g\frac{\partial z}{r\partial\theta}+\frac{\partial}{\partial r}\left[\nu\left(\frac{\partial u}{\partial r}+\frac{u}{r}\right)\right]+\frac{\partial}{r\partial\theta}\left[\nu\left(\frac{\partial u}{r\partial\theta}\right)\right]$$
$$+\frac{\partial}{\partial p}\left[\varkappa\left(\frac{\partial u}{\partial p}\right)\right]+\frac{2}{r^2}\frac{\partial(v\nu)}{\partial\theta} \quad (1)$$

$$\frac{\partial v}{\partial t}+u\frac{\partial v}{r\partial\theta}+v\frac{\partial v}{\partial r}-u\left(\frac{u}{r}+f\right)+\omega\frac{\partial v}{\partial p}$$
$$=-g\frac{\partial z}{\partial r}+\frac{\partial}{\partial r}\left[\nu\left(\frac{\partial v}{\partial r}+\frac{v}{r}\right)\right]+\frac{\partial}{r\partial\theta}\left[\nu\left(\frac{\partial v}{r\partial\theta}\right)\right]$$
$$+\frac{\partial}{\partial p}\left[\varkappa\left(\frac{\partial v}{\partial p}\right)\right]-\frac{2}{r^2}\frac{\partial(u\nu)}{\partial\theta}, \quad (2)$$

$$O=-g\frac{\partial z}{\partial p}-\frac{RT}{p}, \quad (3)$$

$$\frac{\partial u}{r\partial\theta}+\frac{\partial v}{\partial r}+\frac{v}{r}+\frac{\partial\omega}{\partial p}=O, \quad (4)$$

$$H=\left(\frac{\partial T}{\partial t}+u\frac{\partial T}{r\partial\theta}+v\frac{\partial T}{\partial r}+\omega\frac{\partial T}{\partial p}\right)-\frac{RT}{p}\omega. \quad (5)$$

We shall next non-dimensionalize eqs. (1) to (5) by choice of fundamental units L_0, T_0 and p_0 for length, time and pressure respectively. Eqs. (1) to (5) may now be considered as the non-dimensional equations. In Table 2 relations between each of the dimensional and the non-dimensional terms are indicated.

4. On the solutions of the system

The system to be used for numerical calculations will contain certain assumptions. These will be listed below now and we shall hope to give some justification for them.

(i) Steady state, i.e., $\partial u/\partial t=\partial v/\partial t=\partial T/\partial t=O$.

(ii) As a first approximation $-g(\partial z/r\partial\theta)$ is much smaller than other terms in the tangential equation of motion.

(iii) As a first approximation, the friction term $(2/r^2)[\partial(v\nu)/\partial\theta]$ is smaller than other friction terms in the tangential equation of motion.

The system of the equations may now be written as:

$$u\frac{\partial u}{r\partial\theta}+v\left(\frac{\partial u}{\partial r}+\frac{u}{r}+f\right)+\omega\frac{\partial u}{\partial p}$$
$$=\frac{\partial}{\partial r}\left[\nu\left(\frac{\partial u}{\partial r}+\frac{u}{r}\right)\right]+\frac{\partial}{r\partial\theta}\left[\nu\left(\frac{\partial u}{r\partial\theta}\right)\right]$$
$$+\frac{\partial}{\partial p}\left[\varkappa\left(\frac{\partial u}{\partial p}\right)\right], \quad (6)$$

$$u\frac{\partial v}{r\partial\theta}+v\frac{\partial v}{\partial r}-u\left(\frac{u}{r}+f\right)+\omega\frac{\partial v}{\partial p}$$
$$=-g\frac{\partial z}{\partial r}+\frac{\partial}{\partial r}\left[\nu\left(\frac{\partial v}{\partial r}+\frac{v}{r}\right)\right]+\frac{\partial}{r\partial\theta}\left[\nu\left(\frac{\partial v}{r\partial\theta}\right)\right]$$
$$+\frac{\partial}{\partial p}\left[\varkappa\left(\frac{\partial v}{\partial p}\right)\right]-\frac{2}{r^2}\frac{\partial(u\nu)}{\partial\theta}, \quad (7)$$

$$O=-g\frac{\partial z}{\partial p}-\frac{RT}{p}, \quad (8)$$

$$\frac{\partial u}{r\partial\theta}+\frac{\partial v}{\partial r}+\frac{v}{r}+\frac{\partial\omega}{\partial p}=O, \quad (9)$$

$$H=\left(u\frac{\partial T}{r\partial\theta}+v\frac{\partial T}{\partial r}+\omega\frac{\partial T}{\partial p}\right)-\frac{RT}{p}\omega. \quad (10)$$

These equations may be treated as five equations for the five unknowns v, ω, z, T and H if the distribution of u is known. The first assumption, namely that of steady state, is made because our interest here lies in seeing what sort of a system can be obtained by imposing the familiar crescent-shaped geometry of the tangential wind in a mature hurricane. We shall therefore take the data from several mature hurricanes and assume them to be in steady state. The second assumption, namely the neglect of $-g(\partial z/r\partial\theta)$, is made only as a first approximation; it does not mean that the pressure field is symmetric. We shall try and recover the contribution by this term by a method of successive numerical integrations.

It may be mentioned here that in their latest model on hurricanes RIEHL & MALKUS (1961) formulate a symmetric pressure field and this perhaps will justify our neglect of this term as a first approximation. The term $(2/r^2)[\partial(v\,\nu)/\partial\theta]$ is perhaps the smallest of the friction terms because the largest contribution in the tangential equation obviously arises from the radial and perhaps vertical shear of the tangential wind. From existing data on radial winds one can show that this assumption is not at all serious; this assumption, again, is made as a first approximation and its contribution can be recovered by successive numerical integration of the system.

Eqs. (6) and (9) are treated as two equations for the two unknowns v and ω and in principle can yield solutions for v and ω, provided ν and $\varkappa$ are known. Once v and ω are known, one can solve for $-g(\partial z/\partial r)$, since all other terms in eq. (7) are known. If the pressure height $Z(L_0, \theta, p)$ is known at an outer boundary, one can solve for the pressure height $Z(r, \theta, p)$. The hydrostatic equation can be used to solve for $T(r, \theta, p)$. Finally, since all the terms on the right-hand side of eq. (10) are known, one can solve for the distribution of $H(r, \theta, p)$, the non-adiabatic heating.

Next we shall discuss in detail some properties of the equation for the vertical velocity, $\omega(r, \theta, p)$.

We define

$$a = -\frac{\partial u/\partial p}{\dfrac{\partial u}{\partial r} + \dfrac{u}{r} + 2\dfrac{f}{f_0}} \tag{11}$$

and

$$b = -\frac{u\dfrac{\partial u}{r\partial\theta}}{\dfrac{\partial u}{\partial r} + \dfrac{u}{r} + \dfrac{2f}{f_0}} + \frac{\dfrac{\partial}{\partial r}\left\{\nu\left(\dfrac{\partial u}{\partial r} + \dfrac{u}{r}\right)\right\}}{\dfrac{\partial u}{\partial r} + \dfrac{u}{r} + \dfrac{2f}{f_0}} + \frac{\dfrac{\partial}{r\partial\theta}\left\{\nu\dfrac{\partial u}{r\partial\theta}\right\}}{\dfrac{\partial u}{\partial r} + \dfrac{u}{r} + \dfrac{2f}{f_0}} + \frac{\dfrac{\partial}{\partial p}\left\{\varkappa\dfrac{\partial u}{\partial p}\right\}}{\dfrac{\partial u}{\partial r} + \dfrac{u}{r} + \dfrac{2f}{f_0}}. \tag{12}$$

We shall also define a new quantity

$$c = \frac{\partial u}{r\partial\theta}, \tag{13}$$

c being the assymetry term in the continuity equation.

Eq. (6) can be written as

$$v = b + a\omega \tag{14}$$

and the equation of continuity may be written as

$$\frac{\partial\omega}{\partial p} + \frac{1}{r}\frac{\partial vr}{\partial r} + c = O. \tag{15}$$

Eq. (14) and (15) may be combined to eliminate v and we obtain

$$\frac{\partial\omega}{\partial p} + a\frac{\partial\omega}{\partial r} + \frac{\omega}{r}\frac{\partial(ar)}{\partial r} + \frac{1}{r}\frac{\partial(br)}{\partial r} + c = O. \tag{16}$$

Further, let $\quad \dfrac{1}{r}\dfrac{\partial(ar)}{\partial r} = x$

and $\quad -\left(\dfrac{1}{r}\dfrac{\partial(br)}{\partial r} + c\right) = y,$

and we obtain $\quad \dfrac{\partial\omega}{\partial p} + a\dfrac{\partial\omega}{\partial r} + \omega x = y. \qquad (17)$

It will be our aim to solve this equation by the method of characteristics, outlined earlier, in KRISHNAMURTI (1961).

If we let $\quad \dfrac{\delta\omega}{\delta p} = \dfrac{\partial\omega}{\partial p} + a\dfrac{\partial\omega}{\partial r},$

where $\delta\omega$ is a variation in ω along characteristic lines of slope a, then we may write

$$\frac{\delta\omega}{\delta p} + \omega x = y. \tag{18}$$

We notice that we have now exactly the same form of the ω-equation as we had earlier for the symmetric system. We must, however, note the following differences between the symmetric ω-equation and the asymmetric ω-equation (18).

(i) In the symmetric case, no vertical motion was possible without friction. *It is possible to have vertical motions without any friction, this being due to the presence of asymmetries inherent in the prescribed wind field* $u(r, \theta, p)$. The terms responsible for this are $\partial u/r\partial\theta$ in the continuity equation and the term $u(\partial u/r\partial\theta)$ in the tangential equation of motion.

(ii) The tangential wind varies along θ and we have thus contributions from the friction of the asymmetries, i.e.,

$$\frac{\partial}{r\partial\theta}\left(\nu\frac{\partial u}{r\partial\theta}\right).$$

(iii) Since all quantities are now a function of r, θ and p, the characteristic lines will appear different in each plane along which θ is constant.

It may also be noted that the ω-equation for the asymmetric case reduces identically to the ω-equation for the symmetric system, if we drop all terms that depend on $\partial(\ )/\partial\theta$.

An explicit solution for eq. (18) can be written as before

$$\omega(r,\theta,p) = \omega(r,\theta,p_0) + \exp\left(-\int x(r,\theta,p)\,dp\right) \times \int_{p_0}^{p} \exp\left(\int x(r,\theta,p)\,dp\right) \times y(r,\theta,p)\,dp. \quad (19)$$

It appears thus that one would need to draw the characteristic lines for the entire 3-dimensional plane before any calculations could be carried out. A typical set of characteristic lines for a hurricane is illustrated in Fig. 3. One may notice that the lines are very nearly vertical in the lower troposphere. We shall make use of this property in the numerical calculations. We shall assume that the characteristic lines between the 1000 and the 700 mb surfaces are exactly vertical; this is a very valid assumption, because the vertical shear of the wind in a hurricane in the lower troposphere is very nearly zero. We shall show actual data of the tangential winds from several storms and verify this observation. We shall restrict ourselves therefore, and obtain vertical motions between 1000 and 700 mb surfaces only here. The ω-equation can be solved over the entire troposphere by a simple relaxation scheme without use of the method of characteristics, and would be a natural extension of this problem.

5. The details of the numerical calculation of the ω-field

(a) The input data

The actual observations from hurricanes were available at two or three flight levels in most of the cases. Only such storms were selected

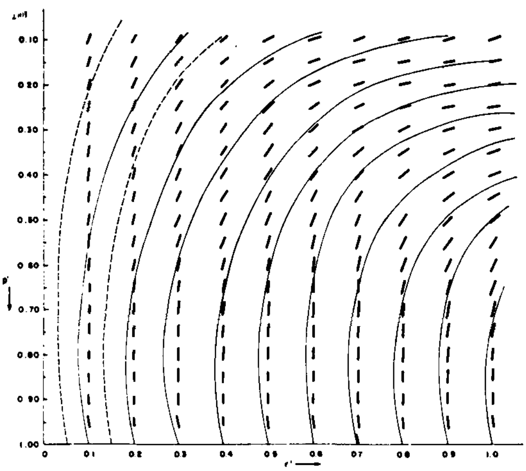

Fig. 3. Typical vertical cross-section of characteristic lines in a hurricane. The scales are expressed in non-dimensional units.

where a good coverage of data for at least two constant pressure levels was available.

We shall propose that a curve fittingin the vertical with a quadratic regression can enable us to obtain a good estimate of $u(r,\theta,p)$. When three levels of data were available at pressures p_1, p_2 and p_3, the following equation was used:

$$u(r,\theta,p) = A(r,\theta)p^2 + B(r,\theta)p + C(r,\theta).$$

Knowing $u(r,\theta,p_1)$, $u(r,\theta,p_2)$ and $u(r,\theta,p_3)$, the three unknowns $A(r,\theta)$, $B(r,\theta)$, and $C(r,\theta)$ can be obtained at each of the grid points. In these storms where only two levels of observations at pressure p_1 and p_2 were available we proposed a maximum tangential wind at the 900 mb surface. We had the following equations:

$$u(r,\theta,p) = A(r,\theta)p^2 + B(r,\theta)p + C(r,\theta)$$

and $$O = 2A(r,\theta)(900) + B(r,\theta).$$

It was thus possible to obtain the three unknowns at each grid point. It may be mentioned, again, that this method appeared very safe, because the tangential wind did not appear to vary much with height in almost all the storms investigated.

All the coefficients $A(r,\theta)$, $B(r,\theta)$ and $C(r,\theta)$ were computed by the IBM 7090 computer at the University of California, Los Angeles, in which these calculations were carried out. We

FIG. 4. Diagram showing the tracks of Hurricanes Daisy and Helene over Atlantic. The dates and positions where flight data were available are marked.

shall next show an analysis of the observed tangential wind for the various storms. The position and the track of these hurricanes are shown in Fig. 4.

(i) *Hurricane Helene, September 26, 1958*

The storm Helene was over the Atlantic and the National Hurricane Research Project flew two complete flights at the 800 and 250 mb surfaces. There was a very good coverage of data and it was easy to obtain a reasonable analysis of the tangential wind field. Figs. 1 and 2 show these fields. The two important features, namely the crescent-shaped geometry and the small vertical variation of the wind are apparent. Actual data is not presented along with the analysis; the reader is referred to JORDAN (1960), where such flight data are shown.

(ii) *Hurricane Daisy, August 25, 1958*

This storm was also over the Atlantic around the same region as Hurricane Helene. Three very complete flights were available for this storm. The storm was just starting to intensify and the maximum winds in the storm were just over 60 knots. Figs. 5, 6 and 7 show the distribution of the tangential wind at the three levels. The familiar features of the hurricane structure were present. At this time the storm was characterized by a secondary wind maxima to the right of the primary one.

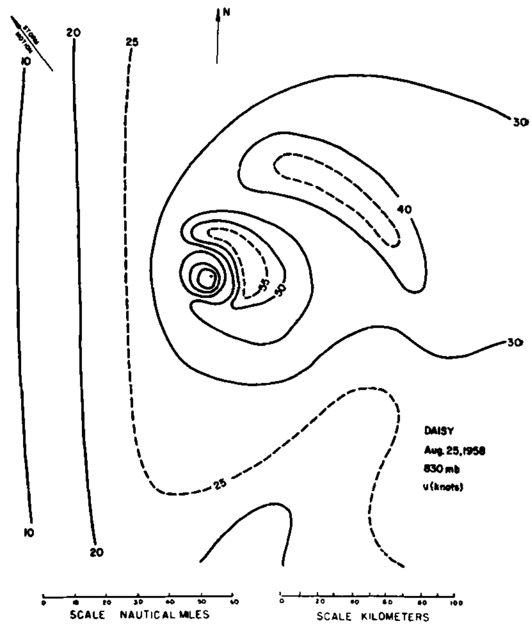

FIG. 5. The tangential wind velocity field in Hurricane Daisy. 830 millibars. Units (knots). August 25, 1958.

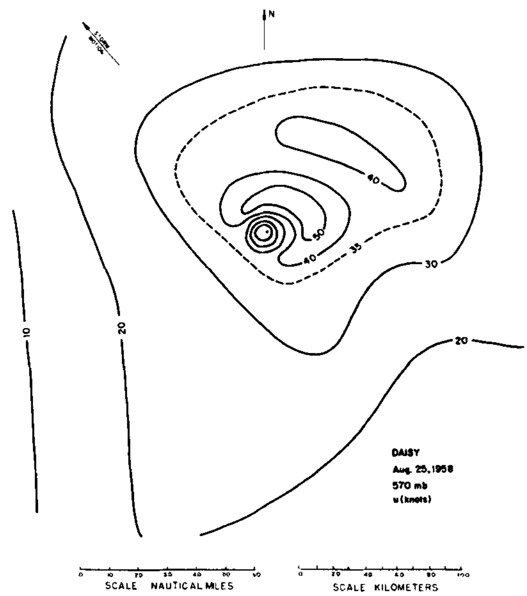

FIG. 6. The tangential wind velocity field in Hurricane Daisy. 570 millibars. Units (knots). August 25, 1958.

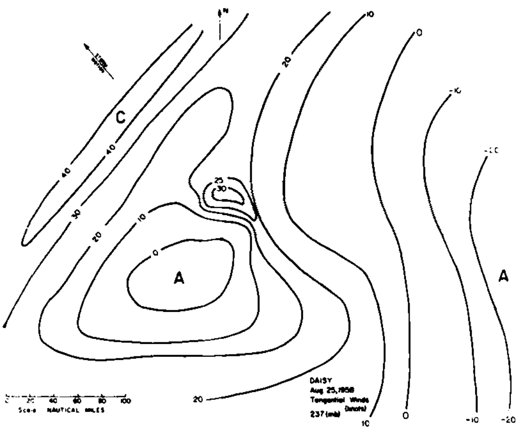

FIG. 7. The tangential wind velocity field in Hurricane Daisy. 237 millibars. Units (knots). August 25, 1958.

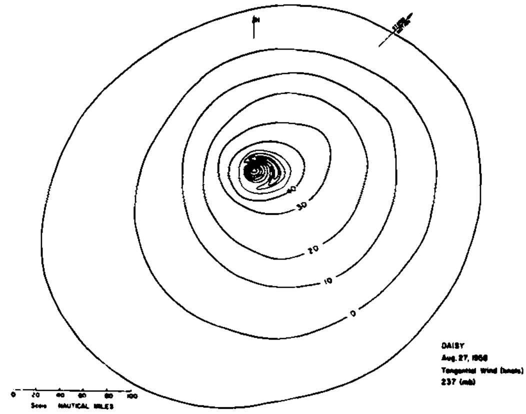

FIG. 9. The tangential wind velocity field in Hurricane Daisy. 237 millibars. Units (knots). August 27, 1958.

(iii) *Hurricane Daisy, August 27, 1958*

On this day two flights were made at the 630 mb and the 237 mb surface. The storm had a wind maximum of over 100 knots. The storm had become nearly steady in its structure at this time. Figs. 8 and 9 show the distribution of the tangential wind.

(iv) *The generalized Rankine vortex*

In addition to the wind field from the actual hurricane, an analytic tangential velocity field was utilized to carry out the same numerical calculations. Our aim here was to find out what sort of vertical motion field was obtained for a generalized Rankine vortex which had a tangential motion field rather similar to that of the hurricane. *Since an analytic solution was also available for this case, it was possible to estimate the errors in the numerical calculations.* We might recall, the Rankine vortex is defined as a one-dimensional vortex for a steady, frictionless motion. From eq. (1) we get

$$\frac{\partial}{\partial r}\left\{v\left(\frac{\partial u}{\partial r}+\frac{u}{r}\right)\right\}=O,$$

which leads to

$$\frac{\partial u}{\partial r}+\frac{u}{r}=\text{a constant},$$

and we get
$$u=ar+\frac{1}{ar},$$

which is the so-called constancy of absolute angular momentum. This is usually called the Rankine vortex. We shall generalize this vortex by writing

$$u(r)=\frac{mar}{1+a^2r^2},$$

which for small r is proportional to ar, and for large r is proportional to $1/ar$. We shall further

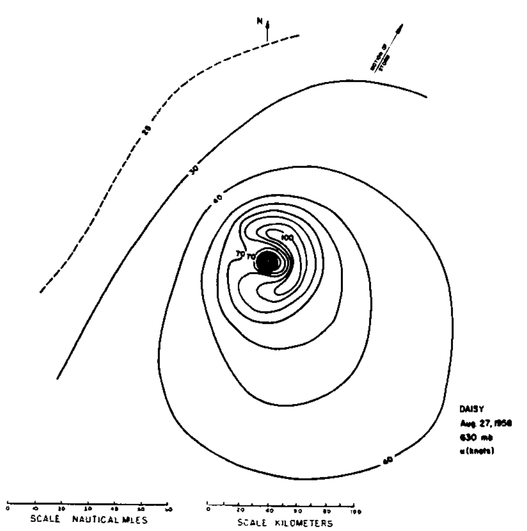

FIG. 8. The tangential wind velocity field in Hurricane Daisy. 630 millibars. Units (knots). August 27, 1958.

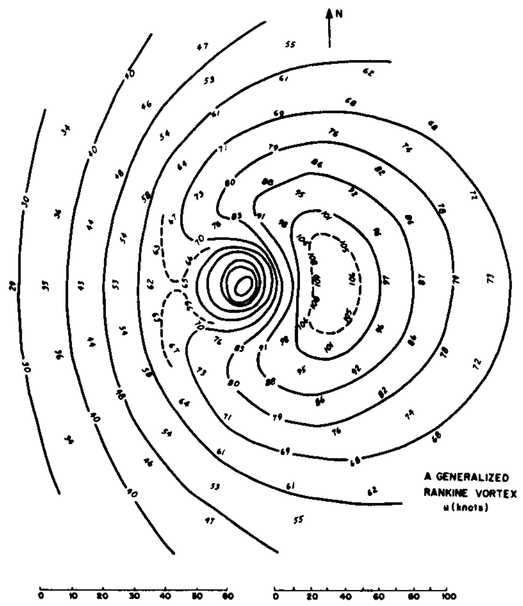

FIG. 10. The tangential wind velocity field for a generalized Rankine vortex, at 900 millibars. Units (knots). Computed from equation 20 of text for values $m = 16.0$, $a = \frac{1}{3}$, and $n = 2$.

add a term ($n \cos\theta$) which will introduce an asymmetry in the wind field. This is equivalent to imbedding the vortex $mar/(1 + a^2 r^2)$ in a current of uniform motion n. Further an artificial vertical variation with height was introduced by multiplying with a function

$$P = \sin \frac{\pi (p - 100)}{1600},$$

where 100 refers to 100 millibars. We had thus

$$u(r, \theta, p) = \left(\frac{mar}{1 + a^2 r^2} + n \cos \theta \right) \sin \frac{\pi (p - 100)}{1600}. \quad (20)$$

This generalized Rankine-type vortex has wind maxima at the 900 mb surface. Fig. 10 shows the tangential wind field $u(r, \theta, 900)$. Our attempt here has been to bring out, as mentioned earlier, the familiar geometry.

(*b*) The grid for calculations

Fig. 11 shows the polar grid used for calculations. Here the following grid distances were used: $\Delta r = 10$ km, $\Delta\theta = 20°$ and $\Delta p = 50$ mb. Wherever derivatives were needed for calculations, centered difference formulas were used over distances $2\Delta r$, $2r\Delta\theta$ and $2\Delta p$ respectively, except at corners, where we used uncentered differences over Δr and Δp respectively.

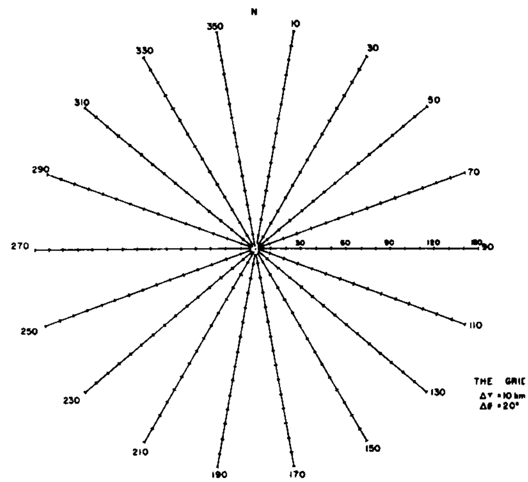

FIG. 11. The polar grid used for numerical calculations. It is centered at the center of the storm position. The grid distances are labelled.

(*c*) The numerical solution of the ω-equation

We shall go back to eq. (19), which gives us the vertical motion $\omega(r, \theta, p)$ as a function of $u(r, \theta, p)$. We had

$$\omega(r, \theta, p) = \omega(r, \theta, p_0) + \exp\left(-\int x(r, \theta, p)\, dp \right)$$
$$\times \int_{p_0}^{p} \exp\left(\int x(r, \theta, p)\, dp \right) y(r, \theta, p)\, dp.$$

It was decided to calculate $x(r, \theta, p)$ and $y(r, \theta, p)$ by the machine at each grid point. We may recall that $x(r, \theta, p)$, being a function of the slope of characteristic lines, is a term independent of the friction coefficients ν and $\varkappa$. At first a calculation of the slope of the characteristic lines, $a(r, \theta, p)$ was made at each grid point. We verified that the slope of the characteristic lines in the lower troposphere between 1000 and 500 mb surfaces was very small, being of the order of 10^{-2}. The term y was divided into several parts. The various parts are as follows:

$$y = y_1 + y_2 + y_3 + y_4, \quad (21)$$

where the asymmetric part of y is:

$$y_1 = -\frac{1}{r}\frac{\partial}{\partial r}\left\{\frac{-u\dfrac{\partial u}{r\partial\theta}}{\dfrac{\partial u}{\partial r}+\dfrac{u}{r}+\dfrac{2f}{f_0}}r\right\} - \frac{\partial u}{r\partial\theta}. \tag{22}$$

The frictional contribution due to radial shear of tangential wind is:

$$y_2 = -\frac{1}{r}\frac{\partial}{\partial r}\left\{\frac{\dfrac{\partial}{\partial r}\left[\nu\left(\dfrac{\partial u}{\partial r}+\dfrac{u}{r}\right)\right]}{\dfrac{\partial u}{\partial r}+\dfrac{u}{r}+\dfrac{2f}{f_0}}r\right\}. \tag{23}$$

The frictional contribution due to tangential shear of tangential wind is:

$$y_3 = -\frac{1}{r}\frac{\partial}{\partial r}\left\{\frac{\dfrac{\partial}{r\partial\theta}\left[\nu\left(\dfrac{\partial u}{r\partial\theta}\right)\right]}{\dfrac{\partial u}{\partial r}+\dfrac{u}{r}+\dfrac{2f}{f_0}}r\right\}. \tag{24}$$

And the frictional contribution due to vertical shear of tangential wind is:

$$y_4 = -\frac{1}{r}\frac{\partial}{\partial r}\left\{\frac{\dfrac{\partial}{\partial p}\left[\varkappa\left(\dfrac{\partial u}{\partial p}\right)\right]}{\dfrac{\partial u}{\partial r}+\dfrac{u}{r}+\dfrac{2f}{f_0}}r\right\}. \tag{25}$$

In writing a machine code for $y(r,\theta,p)$ we obtained outputs for the following combinations of y_1, y_2, y_3, and y_4.

$$\begin{array}{ll} y=y_1 & y=y_1+y_2+y_3 \\ y=y_1+y_2 & y=y_1+y_3+y_4 \\ y=y_1+y_3 & y=y_1+y_2+y_4 \text{ and} \\ y=y_1+y_4 & y=y_1+y_2+y_3+y_4. \end{array}$$

We examined the various combinations in the final distribution of $\omega(r,\theta,p)$ to find the relative importance of each of the terms.

Further, a flexible code was written so that we could examine the distribution of $\omega(r,\theta,p)$ for a wide range of values of ν and $\varkappa$. The code also allowed for variation of ν and $\varkappa$ along the principal coordinates.

(d) Boundary conditions

We shall impose the condition $\omega=0$, at 1000 mb in all our calculations. Since the ω-equation is a partial differential equation of the first order, we have only one boundary condition. Meteorologists working with the diagnostic ω-equation of the quasi-geostrophic vorticity system are familar with two boundary conditions on the vertical motion. The reasons for the differences lie in the fact that the ω-equation (18) is no more than the mass continuity equation, where we have replaced $((\partial v/\partial r)+(v/r))$ by terms involving u and ω. The kinematic method deals with a vertical integration of the horizontal divergence field and also requires one boundary condition. The ω-equation of the quasi-geostrophic vorticity system is a second order equation, because one differentiates the vorticity equation with respect to pressure to eliminate certain time-dependent terms that are common to the vorticity equation and the thermodynamic energy equation. In the system presented here, no further differentiation in the vertical has been made.

6. The results of the computations

The calculations were carried out for the storms mentioned and for the generalized Rankine vortex. Of the various parts of y the only ones that consistently showed significant contributions were y_1 and y_2, namely the vertical motions due to asymmetries in the wind field, and those due to radial shearing stress of the tangential wind. We shall present here the following outputs in each case.

(a) $y=y_1$ (no friction),
(b) $y=y_1+y_2$ (friction due to radial stresses),
(c) $y=y_1+y_2+y_3+y_4$ (complete friction).

We shall also show radar composite charts obtained from aircraft reconnaissance flights made by the National Hurricane Research Project for these storms and make comparisons with the patterns of the computed vertical motions. In the investigation of the symmetric storm, we found that $\nu=\varkappa=0.1$ gave very reasonable distribution of vertical motion. Here again, we are presenting only those results for which $\nu=\varkappa=0.1$. The following dimensional values correspond to these numbers:

$$\nu=2.7\times10^{8}\text{ c.g.s. units,}$$
$$\varkappa=1.2\times10^{7}\text{ c.g.s. units.}$$

In the following drawings not all the figures of the numerical calculations are presented.

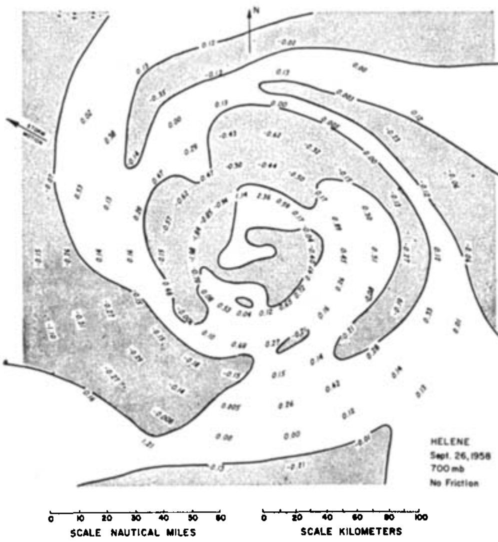

FIG. 12. Non-dimensional vertical velocity field for Hurricane Helene. The results apply for the case $y = y_1$, where none of the friction terms are included. To obtain the vertical velocities in units of millibars/hour, multiply by 131.22.

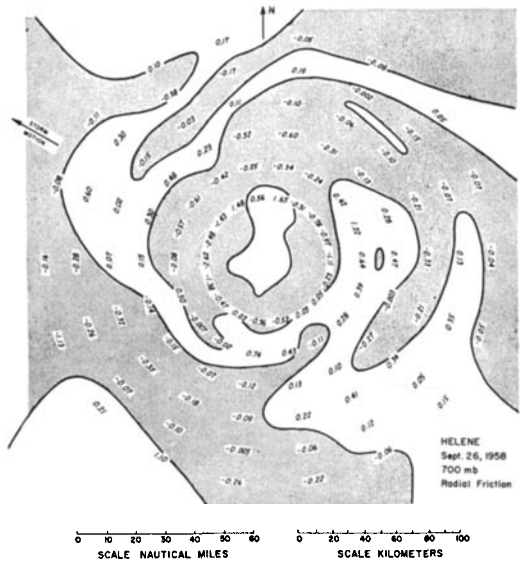

FIG. 13. Non-dimensional vertical velocity field for Hurricane Helene. The results apply for the case $y = y_1 + y_2$, where the friction term due to the radial stress of the tangential wind is included. To obtain the vertical velocity in units of millibars/hour, multiply by 131.22.

(i) *Hurricane Helene, September 26, 1958*

Figs. 12, 13 and 14 show the non-dimensional vertical motion field at the 700 mb surface for this storm. Fig. 12 is obtained for $y = y_1$, the case of no friction. The spiral bands with up and down motion appear due to presence of asymmetries $(\partial u/r\partial\theta)$ and $u(\partial u/r\partial\theta)$ in the input wind field $u(r,\theta,p)$. One may notice that no closed eye wall shows up in this calculation. Fig. 13 is a distribution of the vertical motion field at the 700 mb surface, where $y = y_1 + y_2$, i.e., we have now included in addition the friction term due to the radial stress of the tangential wind. The most interesting feature in this calculation is the presence of an eye with sinking motion. The following additional features may be noted. The largest upward vertical motions are found around the eye. The magnitude of the upward motion falls off rapidly as r increases. The order of magnitude of the vertical motion at $r = 150$ km (100 nautical miles) is one to two orders of magnitude smaller than that near the eye. To obtain the magnitude of vertical motion in units of millibars per hour, the non-dimensional numbers should be multiplied by $p_0 \tfrac{1}{2} f_0 = 131.22$ mb/hr. The magnitudes compare very closely to those the author found for the steady symmetric storm. Fig. 14 shows the

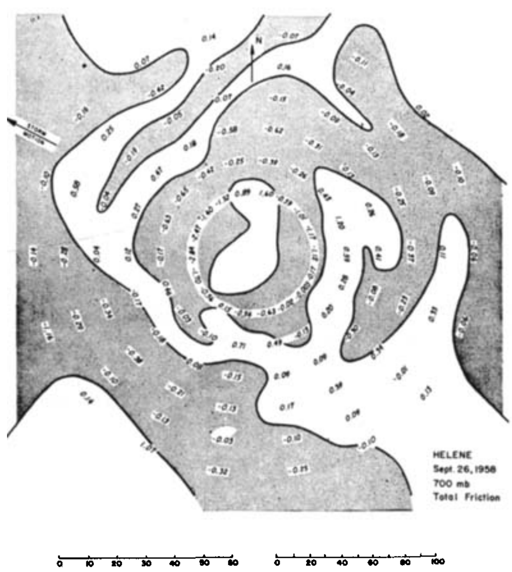

FIG. 14. Non-dimensional vertical velocity field for Hurricane Helene. The results apply for the case $y = y_1 + y_2 + y_3 + y_4$, where all of the friction terms are included. To obtain the vertical velocities in units of millibars/hour, multiply by 131.22.

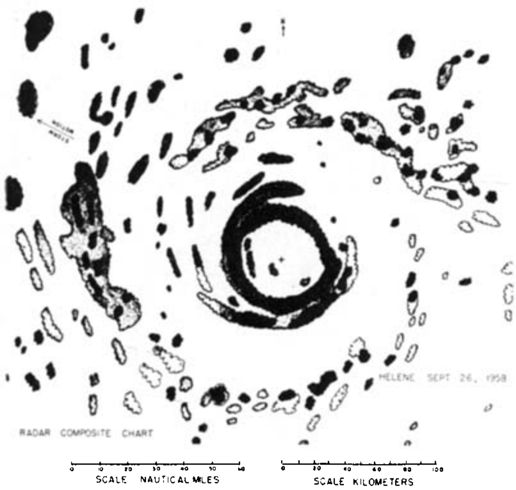

FIG. 15. Radar composite chart for Hurricane Helene. The dark and weaker echoes are shown by different shading. *Note*: Since the 2-cm radar covers a small area, the final picture presented here is not very reliable for $r > 60$ km.

contribution by the complete system, including all of the friction terms. We notice that Figs. 13 and 14 appear rather similar, indicating that the contribution by the friction term y_3 (tangential shear of u) and y_4 (vertical shear of u) are small.

Since y_4 is directly proportional to $\varkappa$, the only way to obtain a larger contribution by this term would be by an increase of $\varkappa$. The value of $\varkappa = 0.1$ is found to be about one to two orders of magnitude too large when compared with the corresponding magnitudes from KASAHARA (1960). It thus appears from this calculation that the vertical shearing stresses do not have an important role in the computed ω-field. The author computed angular momentum exchanges between the ocean and the atmosphere for $\varkappa = 0.1$, and found that there was a significant transfer of absolute angular momentum to the sea surface. This confirms that the role of $\varkappa$, though found important in the surface boundary layer, is perhaps of lesser importance above the layer.

Fig. 15 shows a radar composite chart for the storm Helene obtained on the same day. The reconnaissance aircraft took several pictures along the flight; these were combined into one with respect to the storm center. One sees dark and light echoes in these pictures. A comparison of Figs. 14 and 15 shows very large similarity. The position of the bands of rising motion compare very well with the positions of the echoes. In regions of downward motion there is an absence of echoes. The eye, though a little elongated in shape in the numerical calculations, appears to agree very well with the radar.

(ii) *Hurricane Daisy, August 25, 1958*

Figs. 16, 17, 18 and 19 constitute the corresponding set of drawings for this storm. Most of the results for Hurricane Helene have been duplicated by this calculation. An eye, less well defined, has again appeared by the inclusion of radial frictional stresses. The observed radar and the computed location of the principal spiral bands appear to be in agreement in the overall picture. At this time the storm was intensifying and the terms like $\partial u/\partial t$, $\partial v/\partial t$, $\partial T/\partial t$ were perhaps too large; their omission in the calculations, however, does not appear to distort the final picture much.

(iii) *Hurricane Daisy, August 27, 1958*

The storm had attained constancy in the winds at this time, and the motion of the storm was also very small. Very interesting results were

FIG. 16. Non-dimensional vertical velocity field for Hurricane Daisy. The results apply for the case $y = y_1$, where none of the friction terms are included. To obtain the vertical velocities in units of millibars/hour, multiply by 131.22.

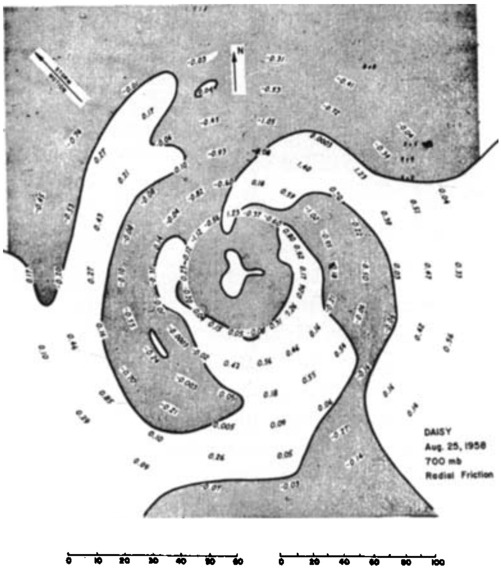

FIG. 17. Non-dimensional vertical velocity field for Hurricane Daisy. The results apply for the case $y = y_1 + y_2$, where the friction term due to the radial stress of the tangential wind is included. To obtain the vertical velocity in units of millibars/hour, multiply by 131.22.

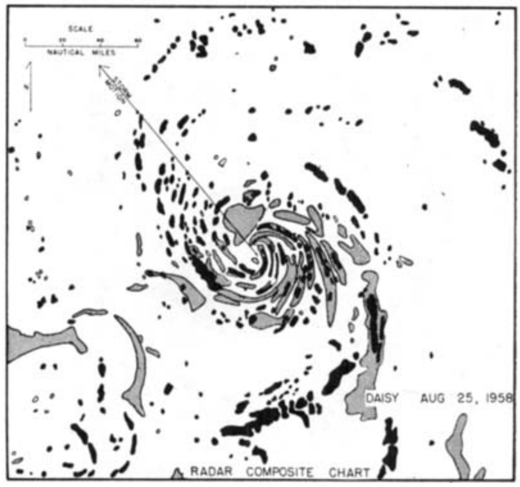

FIG. 19. Radar composite chart for Hurricane Daisy. The dark and weaker echoes are shown by different shading. *Note*: Since the 2-cm radar covers a small area, the final picture presented here is not very reliable for $r > 60$ km.

obtained for this system. Figs. 20 to 23 show the set of drawings. The eye in the radar and in the calculation had an opening. The overall picture is very much in agreement with the radar. And it appears from the presented cases of

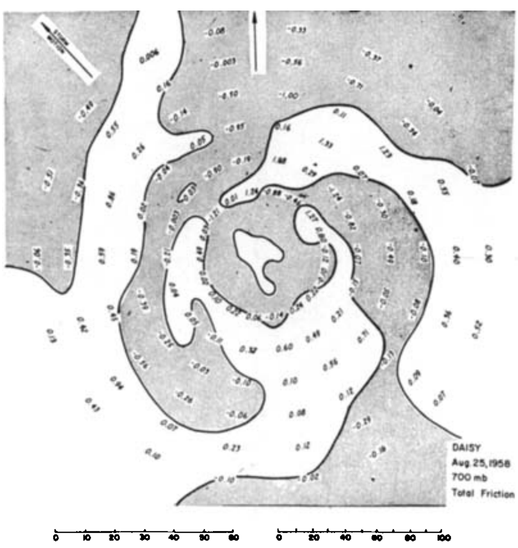

FIG. 18. Non-dimensional vertical velocity field for Hurricane Daisy. The results apply for the case $y = y_1 + y_3 + y_4$, where all of the friction terms are included. To obtain the vertical velocities in units of millibars/hour, multiply by 131.22.

FIG. 20. Non-dimensional vertical velocity field for Hurricane Daisy. The results apply for the case $y = y_1$, where none of the friction terms are included. To obtain the vertical velocities in units of millibars/hour, multiply by 131.22.

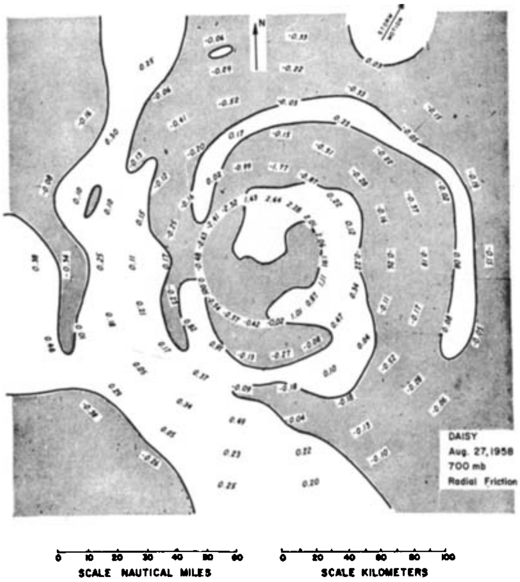

FIG. 21. Non-dimensional vertical velocity field for Hurricane Daisy. The results apply for the case $y = y_1 + y_2$, where the friction term due to the radial stress of the tangential wind is included. To obtain the vertical velocity in units of millibars/hour, multiply by 131.22.

FIG. 22. Non-dimensional vertical velocity field for Hurricane Daisy. The results apply for the case $y = y_1 + y_2 + y_3 + y_4$, where all of the friction terms are included. To obtain the vertical velocities in units of millibars/hour, multiply by 131.22.

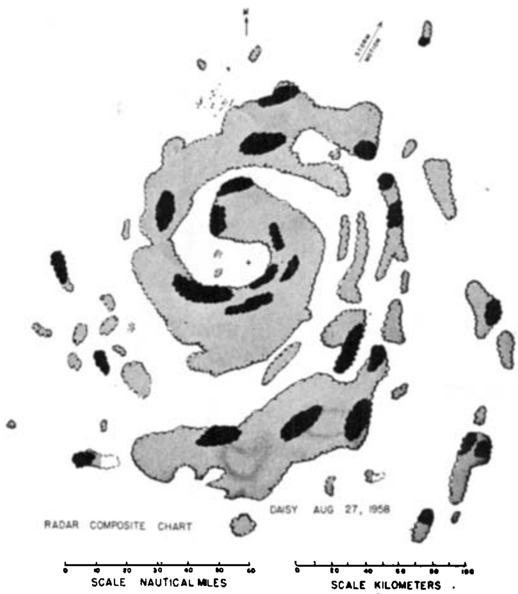

FIG. 23. Radar composite chart for Hurricane Daisy. The dark and weaker echoes are shown by different shading. *Note*: Since the 2-cm radar covers a small area, the final picture presented here is not very reliable for $r > 60$ km.

vertical motion that the ω-equation has the ingredients to give a good description of the vertical motion field.

The magnitude of vertical motion at the 700 mb surface varies from a maximum of 100 to 700 mb/hr near the eye wall to about 1 mb/hr in the outer boundary of the calculations.

(iv) *The generalized Rankine vortex*

In Figs. 24, 25, and 26 we have presented a corresponding set of vertical motion distribution, as obtained by similar finite difference equations.

For the case $y = y_1$ we have the vertical motion due to the simple asymmetry ($n \cos\theta$) in the tangential wind field. The results show a mirror-image of the ω-pattern in the front and the rear quadrants. The places of rising and sinking motion are located in three regions which are placed in a spiral-like form, The $\omega = 0$ line, along $\theta = 0$ and $\theta = \pi$, is perhaps due to the artificial choice of the asymmetry function $n \cos\theta$, that forbids the merging of the three individual regions of upward (and downward) motion into one well-connected spiral. This indeed does appear to be the case, when we examine the analytic solution for this system.

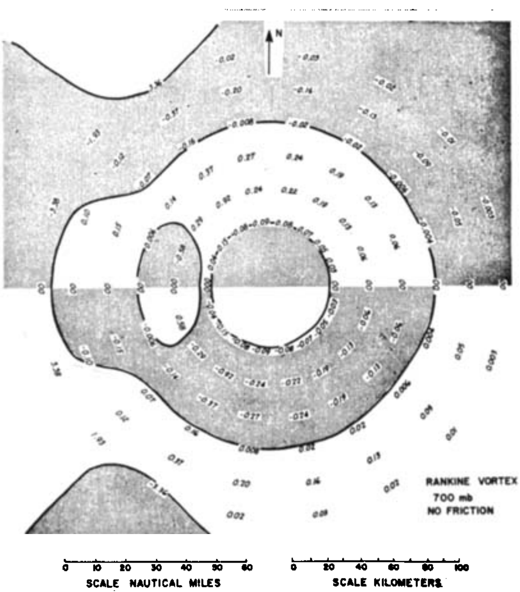

FIG. 24. Non-dimensional vertical velocity field for the generalized Rankine vortex. The results apply for the case $y = y_1$, where none of the friction terms are included. To obtain the vertical velocities in units of millibars/hour, multiply by 131.22.

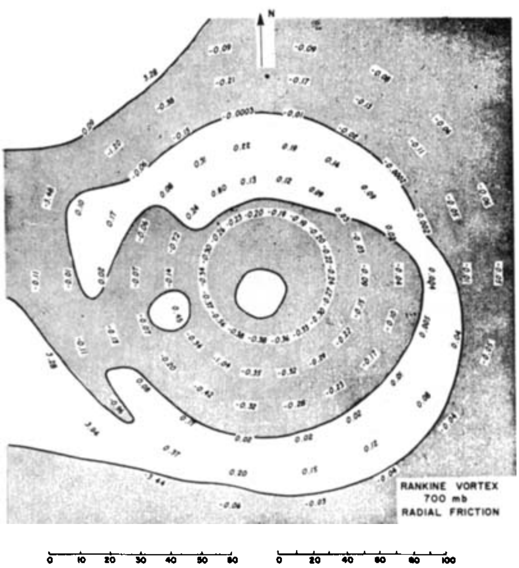

FIG. 25. Non-dimensional vertical velocity field for the generalized Rankine vortex. The results apply for the case $y = y_1 + y_2$, where the friction term due to the radial stress of the tangential wind is included. To obtain the vertical velocity in units of millibars/hour, multiply by 131.22.

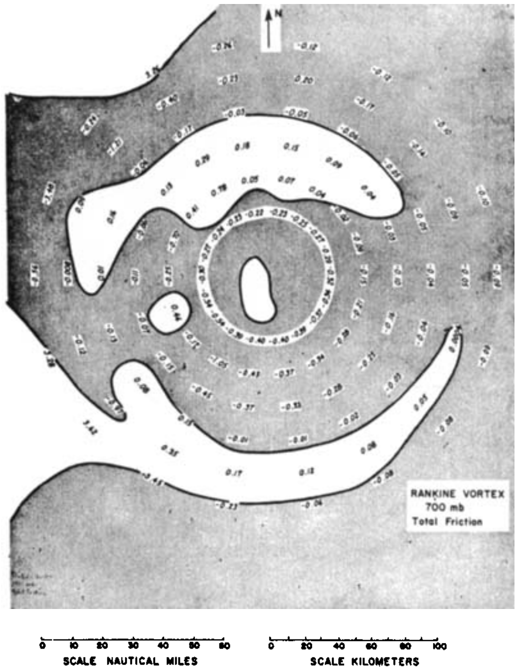

FIG. 26. Non-dimensional vertical velocity field for the generalized Rankine vortex. The results apply for the case $y = y_1 + y_2 + y_3 + y_4$, where all of the friction terms are included. To obtain the vertical velocities in units of millibars/hour, multiply by 131.22.

Fig. 25 shows the results for the case $y = y_1 + y_2$. In this case, the vertical motion field is more spiral. The reason for this lies in the fact that the artificially imposed discontinuity along the lines $\theta = 0$ and $\theta = \pi$ is destroyed by momentum exchange due to radial stresses of the tangential wind. A closed region of sinking motion near the center is obtained in this calculation. Fig. 26 shows the results for $y = y_1 + y_2 + y_3 + y_4$ The final pattern is slightly different from Fig. 25. The magnitude in Figs. 25 and 26 in regions of strong upward and downward motion has not altered. The results thus seem to be similar to those that were obtained for the hurricane.

7. The analytic solution for the generalized Rankine vortex and estimates of numerical errors in the finite difference formulation

Let us assume that the tangential wind distribution in a mature hurricane be given by the expression:

$$u(r,\theta,p)=\{R(r)+\Theta(\theta)\}P(p), \tag{26}$$

where R, Θ and P are functions of r, θ and p respectively.

(*a*) The characteristic lines

For a constant Coriolis parameter $f=f_0$ we have,

$$a(r,\theta,p)=-\frac{\partial u/\partial p}{\dfrac{\partial u}{\partial r}+\dfrac{u}{r}+2}$$

$$=-\frac{(R+\Theta)\dfrac{\partial P}{\partial p}}{P\left(\dfrac{\partial R}{\partial r}+\dfrac{R+\Theta}{r}\right)+2}$$

The slope of the characteristic line in any plane $\theta=\theta_0$ will be given by

$$a(r,\theta_0,p)=\frac{dr}{dp}=\frac{-(R+\Theta_0)\dfrac{\partial P}{\partial p}}{P\left(\dfrac{\partial R}{\partial r}+R+\dfrac{\Theta_0}{r}\right)+2}$$

or
$$\frac{dr}{dP}=\frac{-(R+\Theta)_0}{P\left(\dfrac{\partial R}{\partial r}+\dfrac{R+\Theta_0}{r}\right)+2}. \tag{27}$$

Eq. (27) can be inverted and we obtain

$$\frac{dP}{dr}+Pg(r)=f(\mathrm{r}), \tag{28}$$

where
$$g(r)=\frac{\partial}{\partial r}\{\ln r(R+\Theta_0)\}$$

and
$$f(r)=-\frac{2}{(R+\Theta_0)}.$$

Eq. (28) may be treated as a first-order ordinary differential equation and we can obtain the following solution:

$$P=\frac{1}{(R+\Theta)}\left\{\frac{D}{r}-r\right\}, \tag{29}$$

where D is the integration constant. Eq. (29) is the analytic expression for the characteristic lines of the system (26). Since the exact equation for the characteristic lines is known, it becomes easier to perform integration along this new coordinate.

(*b*) The vertical motion field

Referring back to eq. (19), we shall first obtain an expression for x and $\exp\left(\int x\,dp\right)$. Substituting for $u(r,\theta,p)$, we obtain

$$x=-\frac{\partial R}{\partial r}\frac{\left(\dfrac{\partial P}{\partial p}\right)}{(PL+2)}+(R+\Theta)\frac{\partial L}{\partial r}\frac{\left(P\dfrac{\partial P}{\partial p}\right)}{(PL+2)^2}-\frac{R+\Theta}{r}\frac{\left(\dfrac{\partial P}{\partial p}\right)}{(PL+2)}$$

and

$$\exp\left(\left(\int x\,dp\right)\right)=(PL+2)^{\xi}\exp\left(\frac{\eta}{PL+2}\right), \tag{30}$$

where
$$L=\frac{\partial R}{\partial r}+\frac{(R+\Theta)}{r},$$

$$\xi=-\frac{1}{L}\frac{\partial R}{\partial r}-\frac{(R+\Theta)}{rL}+\frac{(R+\Theta)}{L^2}\frac{\partial L}{\partial r}$$

and
$$\eta=\frac{2(R+\Theta)\dfrac{\partial L}{\partial r}}{L^2}.$$

Considerable difficulties arise in the formulation of $y(r,\Theta,p)$ for the system. An analytic solution was attempted only for the case $y=y_1$. We have

$$y=y_1=-\frac{\partial}{r\partial r}\left(\frac{-u\dfrac{\partial u}{\partial\theta}}{\dfrac{\partial u}{\partial r}+\dfrac{u}{r}+2}\right)-\frac{\partial u}{r\partial\theta};$$

substituting again for $u(r,\theta,p)$ we obtain,

$$y_1=-\frac{1}{r}\frac{\left(P^2\dfrac{\partial\Theta}{\partial\theta}\dfrac{\partial R}{\partial r}\right)}{\left\{P\left(\dfrac{\partial R}{\partial r}+\dfrac{R+\Theta}{r}\right)+2\right\}}+\frac{p^3(R+\Theta)\dfrac{\partial\Theta}{\partial\theta}\left(\dfrac{\partial^2R}{\partial r^2}+\dfrac{1}{r}\dfrac{\partial R}{\partial r}-\dfrac{R}{r^2}\right)}{r\left\{P\left(\dfrac{\partial R}{\partial r}+\dfrac{R+\Theta}{r}\right)+2\right\}^2}-\frac{P}{r}\frac{\partial\Theta}{\partial\theta}. \tag{31}$$

This general expression for y_1 appears rather complicated, but for arbitrary functions $R(r)$, $\Theta(\theta)$ and $P(p)$ an analytic form of y_1 can be derived easily by substitution.

Substituting in the equation for the vertical motion, we get an expression of the form

$$\omega(r,\theta,p) = (PL+2)^{-\xi} \exp\left(-\frac{\eta}{PL+2}\right) \times \int_{1000}^{p} (PL+2)^{\xi} \exp\left(\frac{\eta}{PL+2}\right) y_1 \, dp, \quad (32)$$

where the vertical integration is to be carried out along the characteristic lines of eq. (39). Next we make the following substitution:

$$R(r) = \frac{mar}{1+a^2r^2},$$

where m and a were constants (in the problem, equal to 16.0 and $\frac{1}{8}$ respectively), $\Theta(\theta) = \eta \cos \theta$, where η is a constant ($=2.0$), and

$$P(p) = \frac{\sin \pi (p-100)}{1600}.$$

The complicated form of the integral does not readily yield a solution even for this simplified form of the generalized vortex. A machine calculation of $\eta/(PL+2)$ was made at each grid point to see if we could replace the term $\exp(\eta/(PL+2))$ by a terminating series and thus perform an exact integration for $\omega(r,\theta,p)$. It turned out, however, that the term $\eta/(PL+2)$ exceeds unity for certain values of r. The only other method left at our disposal was to evaluate the magnitude of the integrand exactly at each grid point. We found that the calculation of the integrand between 1000 and 700 mb showed that it had a monotonic variation with pressure. It was then decided to obtain $\omega(r,\theta,p)$ by a simple machine calculation of the integral. Since no space derivatives are involved, we considered the final output to be free of space truncation.

We found that $\omega(r,\theta,p)$ for $y=y_1$ was almost identical to what was obtained by the finite difference grid-network. The calculation showed zero vertical motions along $\theta=0$ and $\theta=\pi$. We were able to understand the reason for this unusual feature from the analytic form of y_1, since $y_1 = (\partial\Theta/\partial\theta) \times$ (function of r,θ,p) as was shown in eq. (31).

For $\Theta = n\cos\theta$ we obtain $y_1 = -n\sin\theta \times$ (function of r,θ,p). Along $\theta=0$ and $\theta=\pi$ this gives $y_1=0$ at all levels and we obtain no vertical motion along these lines. It therefore suggests that $\Theta = n\cos\theta$ is not the proper type of asymmetry that we should associate with the hurricane. It also confirms what has been found by meteorologists earlier (LEON SHERMAN, 1956), that the asymmetry of the wind field in hurricanes is perhaps more than what is obtained when a symmetric vortex is imbedded in a zonal current.

It was unfortunate that we could not carry out the analytic solution exactly all the way; this, as the reader will know, is due to the extreme complexity of the non-linear system of equations.

8. Conclusions and general comments

We have presented here a diagnostic use of the observed tangential wind field in hurricanes. The analysis applies to mature, slowly moving hurricanes.

The neglect of $\partial u/\partial t$, in comparison to terms like uv/r in the scale of calculations ($r \leq 2°$ latitude), is not serious.

The analytic solution for the generalized Rankine vortex shows that the finite difference formulation of the system has very small space truncation. This may be because no time integrations have been carried out. The results apply for one time period. If we had carried out integration on the same grid for an initial-value problem, perhaps space-truncation errors would have built up.

Two possible areas where certain amounts of subjectivity have entered are: the hand analysis of the tangential wind speed and the construction of the radar composite chart. Objective analysis of the aircraft flight data by methods of spectral resolution, using Bessel functions, would perhaps be an improvement in the handling of the input data. The currently used 2 cm wavelength radar could be improved to obtain a larger areal coverage of echoes.

We have shown that, when the crescent-shaped geometry of the tangential wind field in hurricanes is rigorously imposed on the primitive equations of atmospheric motion, the solution for the vertical motion field exhibits spiral bands that very strongly resemble the radar pictures.

With a simple Navier-Stokes formulation of the friction terms, it is possible to reproduce features like the eye and the eye wall. This is obtained by the friction term that depends on the radial stress of the tangential wind. The other friction terms do not appear to be important in the resolution of the vertical motion field.

The results presented here apply at the 700 mb surface. We propose to continue this work and solve the ω-equation by a simple relaxation procedure between 1000 and 100 mbs. We shall present the complete 3-dimensional structure of all the variables v, ω, z, T and H, as obtained by numerical integration of the system of equations. It will be hoped that this diagnostic use of the tangential wind will enable us to understand the dynamics of the hurricane.

Acknowledgements

The author wishes to express his appreciation to Mr. Harry F. Hawkins, Director of the National Hurricane Research Project at Miami, Florida, for providing all the reconnaissance flight data presented here.

This work was in part supported by grants from the National Science Foundation, N.S.F. Grant 9501, and the Institute of Geophysics, University of California.

The author would like to thank Professors M. G. Wurtele, M. Neiburger and J. Bjerknes for discussions on various aspects of this work.

He would also like to thank Mr. William M. Gray, of Colorado State University, Dr. J. Malkus, University of California, and Captain J. Bekius, U.S.A.F., of the University of California, for providing the radar-composite charts.

Appreciation is also expressed to the Western Data Processing Center and the Numerical Analysis Research Center for providing the facilities of the IBM 7090 at the University of California, Los Angeles, for carrying out the numerical calculations.

REFERENCES

BERKOFSKY, L., 1960, A numerical model for the prediction of hurricane formation. *Geophysics Research Papers No.* 67.

JORDAN, C. L., and *collaborators*, 1960, On the structure of Hurricane Daisy on 27 August 1958. *J. Meteor.*, 17, pp. 337–348.

KASAHARA, A., 1960, *A Numerical Experiment on the Development of a Tropical Cyclone.* Technical Report. Department of Meteorology, University of Chicago.

KRISHNAMURTI, T. N., 1961, On the vertical velocity field in a steady symmetric hurricane. *Tellus*, 13, pp. 171–180.

KUO, H. L., 1959, Dynamics of convective vortices and eye formation. *The Rossby Memorial Volume.* Rockefeller Institute Press, New York.

PALMEN, E., and RIEHL, H., 1957, Budget of angular momentum and energy in tropical cyclones. *J. Meteor.*, 14, pp. 150–159.

RIEHL, H., and MALKUS, J. S., 1961, Some aspects of Hurricane Daisy. *Tellus* 13, pp. 181–213.

SHERMAN, L., 1956, On the wind asymmetry of hurricanes. *J. Meteor.*, 13, pp. 500–503.

WEXLER, H., 1947, Structure of hurricanes as determined by radar. *N.Y. Acad. Sci., Annals*, 48, p. 821.